NEOPLASIA
www.neoplasia.com

Volume 11 Number 7 July 2009 pp. 700–711 700

Aberrant Methylation and Reduced Expression of LHX9 in Malignant Gliomas of Childhood[1]

Valentina Vladimirova*, Thomas Mikeska*,†, Andreas Waha*, Niels Soerensen‡, Jingying Xu§, Patrick C. Reynolds§ and Torsten Pietsch*

*Department of Neuropathology, University of Bonn Medical Center, Bonn, Germany; †Department of Pathology Peter MacCallum Cancer Centre, Melbourne, Australia; ‡Department of Pediatric Neurosurgery, University of Wuerzburg, Wuerzburg, Germany; §USC-CHLA Institute for Pediatric Clinical Research, Children Hospital Los Angeles and The University of Southern California Keck School of Medicine, Los Angeles, CA, USA

Abstract

High-grade gliomas (HGGs) of childhood represent approximately 7% of pediatric brain tumors. They are highly invasive tumors and respond poorly to conventional treatments in contrast to pilocytic astrocytomas, which usually are well demarcated and frequently can be cured by surgery. The molecular events for this clinical relevant finding are only partially understood. In the current study, to identify aberrantly methylated genes that may be involved in the tumorigenesis of pediatric HGGs, we performed a microarray-based differential methylation hybridization approach and found frequent hypermethylation of the *LHX9* (human Lim-homebox 9) gene encoding a transcription factor involved in brain development. Bisulfite genomic sequencing and combined bisulfite restriction analysis showed that HGGs were frequently methylated at two CpG-rich *LHX9* regions in comparison to benign, nondiffuse pilocytic astrocytomas and normal brain tissues. The *LHX9* hypermethylation was associated with reduced messenger RNA expression in pediatric HGG samples and corresponding cell lines. This epigenetic modification was reversible by pharmacological inhibition (5-aza-2′-deoxycytidine), and reexpression of *LHX9* transcript was induced in pediatric glioma cell lines. Exogenous expression of *LHX9* in glioma cell lines did not directly affect cell proliferation and apoptosis but specifically inhibited glioma cell migration and invasion *in vitro*, suggesting a possible implication of *LHX9* in the migratory phenotype of HGGs. Our results demonstrate that the *LHX9* gene is frequently silenced in pediatric malignant astrocytomas by hypermethylation and that this epigenetic alteration is involved in glioma cell migration and invasiveness.

Neoplasia (2009) 11, 700–711

Abbreviations: CGI, CpG island; DMH, differential methylation hybridization; COBRA, combined bisulfite restriction analysis; cRT-PCR, competitive reverse transcription–polymerase chain reaction; 5-aza CdR, 5-aza-2′-deoxycytidine; WHO, World Health Organization; HGG, high-grade glioma; PA, pilocytic astrocytoma

Address all correspondence to: Valentina Vladimirova, PhD or Torsten Pietsch, MD, PhD, Department of Neuropathology, University of Bonn Medical Center, Sigmund-Freud-Str. 25, D-53105 Bonn, Germany. E-mail: valentina.vladimirova@ukb.uni-bonn.de; t.pietsch@uni-bonn.de

[1]This study was supported by National Genome Research Network NGFN2, Brain Tumor Net (grant 01GS0461; N3KRS04T01), the SMP Epigenetics PEG-S04T02, the Kinderkrebsstiftung (grant DKS 2006.03), German Ministry for Education and Research BMBF, Competence Network Pediatric Oncology and Hematology, Project Embryonal Tumors (grant 01GI0418), and BONFOR program of the Medical Faculty of the University of Bonn.
Received 28 February 2009; Revised 8 April 2009; Accepted 9 April 2009

DOI 10.1593/neo.09406

Introduction

High-grade astrocytomas (World Health Organization [WHO] grades 3 and 4) are considered to derive from astrocytic precursor cells. Malignant anaplastic astrocytoma and glioblastoma of childhood are infrequent compared with their adult counterparts and comprise approximately 7% of pediatric brain tumors [1]. Although the survival rates have increased during the recent years, especially because of better surgical techniques and postoperative treatment, the prognosis is still poor compared with nondiffuse pilocytic astrocytomas (PAs; WHO grade 1), which usually are demarcated and frequently can be cured by surgery.

Carcinogenesis, in general, is a multiple-step process that may involve both genetic and epigenetic changes. Alterations of DNA methylation seem to be early events and occur more frequently than individual genetic changes [2]. Epigenetic changes especially DNA methylation of the promoter CpG islands (CGIs) and consequent gene silencing are important processes for both initiation and progression of human cancers. Aberrant methylation of CGI-associated promoter regions of genes is a frequent epigenetic event in tumor cells accompanied by alterations in histone modification and chromatin conformation rendering the CGI and its associative promoter transcriptionally inert [3]. Such epigenetic modifications have been reported to be widespread and likely contribute to gliomagenesis [4,5]. For example, in human gliomas, epigenetic alterations are implicated in the silencing of genes involved in the regulation of cell cycle (*RB*, *p16INK4A*, *p73*), DNA repair (*MGMT*), apoptosis (*DAP* kinase 1), angiogenesis (*THBS1*), and invasion (*TIMP3*) [6].

Differential methylation hybridization (DMH) is one of the global techniques developed to analyze alterations of DNA methylation in human cancer using CGI microarrays [7]. In the current study, we applied DMH to identify aberrantly methylated genes that may be involved in tumorigenesis of pediatric high-grade gliomas (HGGs) and found frequent hypermethylation of *LHX9*, LIM-homeodomain (LIM-hd) 9 transcription factor, which belongs to a family of developmental regulators. It is expressed in embryonic mouse brain, with the highest level of expression in the diencephalon, telencephalic vesicles, and dorsal mesencephalon [8]. The expression pattern and structural characteristics of *LHX9* suggest that it encodes a transcription factor that might be involved in the control of cell differentiation of several neural cell types [9]. The DNA methylation status of human *LHX9* has not been previously analyzed. In this study, we describe for the first time that *LHX9* is frequently inactivated in malignant astrocytomas and glioma cell lines by the hypermethylation of the CGI-associated region within the gene compared with benign pediatric PAs and normal brain tissue samples. The hypermethylation is associated with a reduced expression of *LHX9* and can be restored after treatment with a demethylating agent. Functional analyses suggest that *LHX9* silencing is specifically involved in the migratory and invasive potential of pediatric malignant gliomas.

Materials and Methods

Glioma Samples and Cell Lines

Glioma samples were obtained from 39 pediatric (aged ≤18 years) patients and were classified according to the WHO classification criteria using histological and immunological methods [10]. The tumor series included 14 PAs, WHO grade 1, 14 anaplastic astrocytomas WHO grade 3, and 11 glioblastoma multiforme (GBM) WHO grade 4. The pediatric patients have been enrolled in the multicenter treatment study for pediatric malignant brain tumors of the German Society of Pediatric Oncology and Hematology (HIT-GBM) [11]. Biopsies of the white matter of brain of three pediatric patients with epilepsy or congenital malformations were included as nonpathological controls. The study was approved by the ethics committee of the University of Bonn Medical Center. To exclude contaminations by normal or necrotic tissues, frozen tissue materials were selected for DNA and RNA extractions after careful examination of corresponding hematoxylin-eosin–stained sections. All samples selected contained at least 80% of vital tumor.

The glioma cell line CHLA-200 was derived from an 8-year-old patient with anaplastic astrocytoma (Xu and Reynolds, unpublished observations) and was kindly provided by Dr. Reynolds from USC-CHLA Institute for Pediatric Clinical Research, Los Angeles. CHLA-200 cells were cultured in Iscove's modified Dulbecco's medium (Invitrogen, Karlsruhe, Germany) supplemented with 20% fetal calf serum (FCS; Invitrogen), 2 mM L-glutamine and human insulin-transferrin–selenous acid solution (Invitrogen). Cell lines KNS-42 derived from a 16-year-old patient with glioblastoma and KG-1-C derived from a 13-year-old patient with mixed glioma were purchased from the Japanese Collection of Research Bioresources and Health Science Research Resources Bank, whereas the SF188 cell line derived from an 8-year-old patient with glioblastoma was obtained from the UCSF/Neurosurgery Tissue Bank. Cells were cultured in Dulbecco's modified Eagle medium (Invitrogen) supplemented with 10% FCS and 2 mM L-glutamine. All cell lines were maintained at 37°C in a 5% CO_2 atmosphere.

DNA samples derived from normal testis tissues were kindly provided by Dr. K. Biermann, Department of Pathology, University of Bonn.

DNA and RNA Extraction

Genomic DNA was obtained from frozen tissues by standard proteinase K digestion and phenol-chloroform extraction and from glioma cell lines using QIAamp DNA Mini tissue Kit (Qiagen, Duesseldorf, Germany). Total RNA from frozen tissue samples and cell lines was isolated using TRIZOL reagent (Invitrogen) according to the manufacturer's instructions. To remove any contaminating genomic DNA, the total RNA was digested with 10 U of RNase-free DNase (Promega, Mannheim, Germany) and 40 U of RNasin (Promega) in a volume of 30 μl before reverse transcription. The RNA was reverse-transcribed using the Superscript II Preamplification System (Invitrogen) with random hexamers as primers in a final volume of 20 μl.

Differential Methylation Hybridization Analysis and CGI Identification

The DMH procedure was performed as described [12]. CpG-rich DNA fragments were isolated from the human CGI library and screened for the presence of *Bst*UI and *Hpa*II (New England Biolabs GmbH, Frankfurt, Germany) restriction sites. Sixteen thousand suitable fragments were polymerase chain reaction (PCR)–amplified using plasmid primer and spotted onto UltraGAPS microarrays (Corning, Acton, MA). For amplicon generation, 2 μg of genomic DNA derived from nine pediatric malignant astrocytic tumors and a pool of control DNA obtained from the white matter of three pediatric brain tissue samples were digested with *Mse*I (New England Biolabs). After ligation of linkers H12/H24 (New England Biolabs), fragments were digested with methylation-sensitive restriction endonucleases *Bst*UI and *Hpa*II and amplified for 20 cycles with H24 as a primer. Polymerase chain reaction fragments were labeled with the Alexa Fluor 555 (normal brain) and Alexa Fluor 647 (tumor) dyes using the BioPrime Plus Array CGH Indirect Genomic Labeling Kit (Invitrogen). Equal amounts of the labeled and purified amplicons and 10 μg of human Cot-1 DNA

(Invitrogen) were cohybridized on DMH microarrays. Hybridization and analysis were carried out as described [7]. Data from single-copy sequences were normalized, and loci with an Alexa Fluor 647/Alexa Fluor 555 ratio greater than 2.5 were empirically scored as hypermethylated.

The DMH strategy provided information on a CGI-associated region that comprised 3 intron/4 exon within *LHX9* transcript variant 2 (GenBank accession number NM_001014434). CpG island at the 5′-putative promoter region of *LHX9* was identified using a CGI searcher program (http://www.ebi.ac.uk/emboss/cpgplot/) and predicted to possess promoter or enhancer activity using Promoter 2.0 prediction program [13].

Bisulfite Modification and Genomic Sequencing

Bisulfite modification of 500 ng of genomic DNA obtained from tissue samples and cell lines was performed using the EpiTect Bisulfite Kit (Qiagen) according to the manufacturer's instructions. The sequences of the primers used for amplification of the 5′-*LHX9* putative promoter region are listed in Table 1. Polymerase chain reaction was done with 2 μl of bisulfite-treated DNA in a final volume of 30 μl containing PCR buffer, 0.5 μM of each primer, 200 μM of each dNTP, 2 mM $MgCl_2$, and 2.5 U Platinum Taq DNA polymerase (Invitrogen). The 339-bp product containing 22 CpG methylation sites was separated on a 2.5% agarose gel, purified using a QIAquick Gel Extraction Kit (Qiagen), and cloned with the pGEM-T Vector System Kit (Promega). Colony PCR was performed on 8 to 10 white colonies to validate the insert. The obtained PCR products were sequenced by GATC-Biotech AG (Konstanz, Germany) and analyzed by BiQ Analyzer Software [14].

Combined Bisulfite Restriction Analysis

The 5′ CGI-associated putative promoter region (*LHX9* region 1) and CpG-rich fragment within the *LHX9* gene (*LHX9* region 2; Figure 1*A*) were quantitatively analyzed by combined bisulfite restriction analysis (COBRA) in 39 pediatric gliomas including those tissue samples which have been examined by DMH and four glioma cell lines. Nonpathological brain tissue samples were used as controls. The bisulfite-converted DNA were used for a single amplification of the *LHX9* region 1. A nested PCR was set up to amplify the *LHX9* region 2. Polymerase chain reaction products generated with *LHX9* primers (sequences are listed in Table 1*A*) specific for bisulfite-converted DNA as well as *Sss*I-modified genomic DNA used as a fully methylated control were digested with the restriction endonuclease *Bst*UI (5′-CGCG-3′) for *LHX9* region 1 or a combination of two endonucleases *Bst*UI and *Taq*$^{\alpha}$I (5′-TCGA-3′; New England Biolabs) for the second *LHX9* fragment, and subsequently separated on a 4% agarose gel as

Table 1. Sequences of the (A) Two CpG-rich Regions of *LHX9* Analyzed and (B) Primers Used for Amplification Reactions.

A

LHX9 region 1

TTTTTGGTTTGTTTTTTATTGATTTTAAATTGTATGGcgGAGTTTGTGGGTTAGGcgTGGAGGcgGTATTTATTTTTAcgTGT
TTTATATGTAGTAGTAATTTTA**cgcg**GTTTTcgTAAGcgGTTGGGAGGTAAGcgGGcgTTTTTTTATATTTTTTTTTTATTGc
gTTTTGGATTTAcgTTAcgTATcgTTAAGGAGTAcgTGGAGGAGGGGcgGGTAGGTAGGGcgGTATTATTATcgGGATTAGTA
TTTTGGAAcgGTTAATTTTATTGTTTATATTTTTTTTTTTATcgG**cgcg**GGAG***TTTTGTTGTAATTTTTTGTTATTTT***

LHX9 region 2

AGGTTTTTTGTGTAGAGATGTGTTcgTTGTTATTTTGGTATTTTcgTTTcgGAGATGGTTATG**cgcg**T**TcgA**GATTTTGTTTA
TTATTTGAGTTGTTTTATT***TGTTTTATTTGTAATAAGATTTTGATT***AcgGGcgATTATTTcg***GTATGAAGGATAGTTTGGTGT***
ATTGT**cgcg**TTTATT**TcgA**GATTTTTTTGTAAGGAGAGTATTTATcgTAGTTGAGTTATAcgGAGTTGGcgGTTAAGAGcgGc
gGTTTGGTTTTGTTTTATTTTAAcgGTAcgGGTATcgTGTAGAAAGGGcgGTTTcgGAAGcgGAAGAGTTTAGcgTTGGGAGT
GGATATcgTT***AATTATAATTTAGGTGTGTTTTTTAT***

B

Gene	Forward primer (5'-3')	Reverse primer (5'-3')	Product size
bis-LHX9-region1	TTTTTGGTTTGTTTTTTATTGATT	AAAATAACAAAAAATT ACAACAAAA	339bp
bis-LHX9-region2a	AGGTTTTTTGTGTAGAGATGTGTT	AATACACCAAACTATCCTTCATACC	169bp
bis-LHX9-region2b	TGTTTTATTTGTAATAAGATTTTGATT	ATAAAAAACACACCTAAATTATAATT	266bp
LHX9	GCCAAGGACGGTAGCATTTA	TTGCAAGAGGGTCTCGAAGT	240bp
LHX9-T7-DEL	*GGATCCTAATACGACTCACTATAGGGAGG* GCCAAGGACGGTAGCATTTA	TTGCAAGAGGGTCTCGAAGT↓ TCCTTCATGCCGAAATGGTC	220bp
b-actin	GATTCCTATGTGGGCGACGAG	CCAGACGCAGGATGGCATGG	384bp
b-actin-T7-DEL	*GGATCCTAATACGACTCACTATAGGGAGG* GATTCCTATGTGGGCGACGAG	CCAGACGCAGGATGGCATGG↓ GGAGTCCATCACGATGCCAGT	334bp
PCDH-gamma-A11	CAAAGATTCAGGCCAGAACG	CCAAGATCATGGCTTGCAGC	227bp

(A) Sequences of the CpG-rich regions of *LHX9* gene showing the positions of CpG sites (cg) in gray and the primers (bold italic) used for amplification after bisulfite treatment of genomic DNA. The *Bst*UI (5′-CGCG-3′) and *Taq*$^{\alpha}$I (5′-TCGA-3′) restriction sites are boxed. (B) Sequences of the primers (bis-) used for amplification of bisulfite-modified genomic DNA and the primers used for the cRT-PCR, which were always chosen to span at least 1 intron. The cRT-PCR was described in the Materials and Methods section using T7-forward primer (italic) and deletion reverse primer. Arrow in the sequence of the deletion reverse primer (DEL) indicates the deletion.

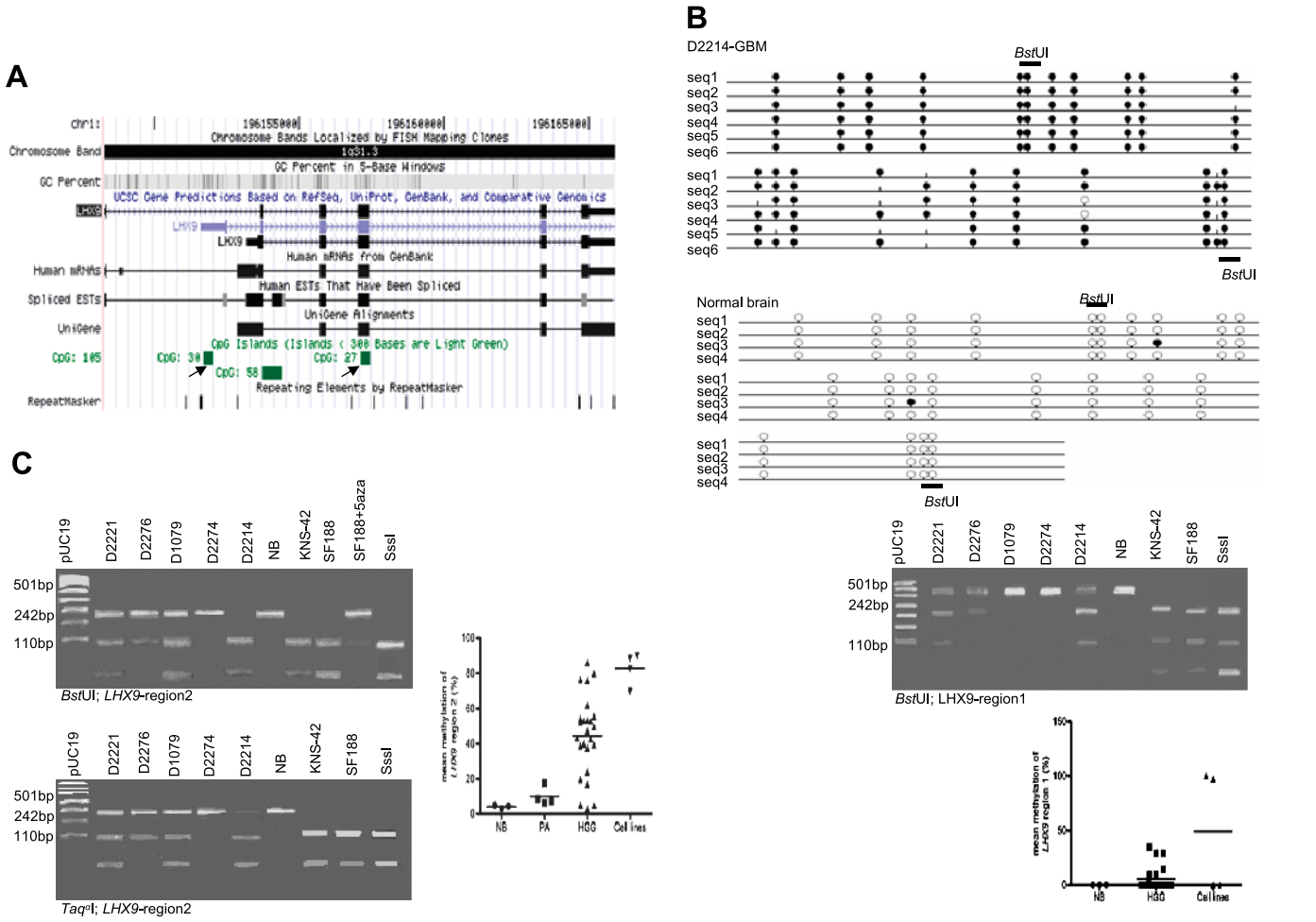

Figure 1. Methylation profile of the two CpG-rich fragments of *LHX9* gene in pediatric HGGs, PAs, and glioma cell lines. (A) Schematic structure of the *LHX9* gene including its chromosomal mapping, mRNA, and CGI content. Arrows indicate the positions of the two CpG-rich regions analyzed by bisulfite sequencing or COBRA approaches. (B) Lollipop-style representation of the methylation status of 22 CpG residues within the *LHX9* CGI-associated putative promoter region 1 of one pediatric HGG (D2214-GBM) and one normal brain tissue sample. Filled (black) circles define methylated CpG site, open (white) circles display unmethylated CpG, and vertical lines without a circle correspond to a single nucleotide polymorphism affecting one of the contained CpG sites. *Bst*UI restriction sites (bold lines) are also indicated. Methylation level of the *LHX9* region 1 was also estimated by COBRA. The PCR products from bisulfite converted DNA samples were digested with restriction endonuclease *Bst*UI (see Materials and Methods). Picture of agarose gel electrophoresis represents the methylation profile of five HGGs, one normal brain control sample, and two cell lines. Scatter plot summarizes the methylation level of *LHX9* region 1 in 25 HGG and 4 glioma cell lines. Seven cases (28%) were methylated and quantified to an average of 20% methylated alleles comparing with the three nonpathological tissue samples which were unmethylated. Two (50%) of the cell lines were hypermethylated. (C) Methylation levels of the CpG-rich *LHX9* region 2 were estimated by COBRA using a combination of two restriction endonucleases *Bst*UI and *Taq*$^{\alpha}$I (see Materials and Methods). The methylation status of five HGGs and two glioma cell lines is shown. Scatter plot summarizes the methylation profile of *LHX9* region 2. Of 25 HGGs, 22 (88%) were aberrantly methylated and quantified to an average of 51% methylated alleles; 4 (29%) of 14 PAs showed a low level of methylation and quantified to an average of 10% methylated alleles compared with the unmethylated normal brain control samples. The four cell lines were hypermethylated. The degree of methylation of each sample was determined as a ratio of the signal intensity of the digested bands to that of all bands. *Sss*I-treated genomic DNA was used as a fully methylated control. The COBRA approach also showed methylation level of the *LHX9* region 2 in SF188 cells before and after treatment with the demethylating agent 5-aza CdR (SF188 + 5aza).

described previously [15]. The *LHX9* region 1 amplicon contains two *Bst*UI restriction sites, whereas the overlapping *LHX9* region 2 products have one *Bst*UI and one *Taq*$^{\alpha}$I restriction sites (Table 1*A*). If *LHX9* region 1 is unmethylated, the 339-bp PCR product remains intact, whereas if it is methylated, this band is digested to 201-, 107-, and 31-bp products. If *LHX9* region 2 is unmethylated, both 169- and 266-bp amplicons remain intact, whereas if it is methylated, the 169-bp band is digested with *Bst*UI to 65- and 104-bp products or with *Taq*$^{\alpha}$I to 70- and 99-bp products and the 266-bp band is digested with *Bst*UI to 71- and 195-bp products or with *Taq*$^{\alpha}$I to 81- and 185-bp products. The degree of DNA methylation of each sample was determined as a ratio of signal intensity of the digested bands to that of all bands.

Treatment of Glioma Cells with Demethylating Agent

Glioma cell lines CHLA-200, SF188, and KNS-42 were grown in the presence or absence of the demethylating agent 5-aza-2′-deoxycytidine (5 μM 5-aza CdR; DNA methyltransferase inhibitor; Sigma-Aldrich, Hannover, Germany) for 4 days. The medium was replaced daily.

Total RNA was isolated from 1×10^6 cells using TRIZOL reagent (Invitrogen), and the *LHX9* messenger RNA (mRNA) expression levels were analyzed by competitive reverse transcription–PCR (cRT-PCR). The *PCDH-γ-A11* gene (protocadherin-gamma subfamily A11), which is known to be silenced by methylation in astrocytoma cells [16], was used to verify the effect of 5-aza CdR treatment in our experiments.

Competitive RT-PCR Analysis

Total RNA was reverse-transcribed using the Superscript II Preamplification System (Invitrogen). Polymerase chain reaction was set up with *LHX9* and *β-actin* specific primers (Table 1*B*) resulting in amplicons of 240 bp for *LHX9* and 384 bp for *β-actin*. RNA competitor molecules with internal deletions for *LHX9* and for the housekeeping gene *β-actin* were generated by *in vitro* mutagenesis and *in vitro* transcription as described [17]. The sizes of the mutated competitor PCR products were 220 bp for *LHX9* and 334 bp for *β-actin*. For cRT-PCR, predetermined amounts of homologous exogenous competitor RNA (from 0.8 to 150 pg) and 250 ng of total RNA were reverse-transcribed. Polymerase chain reaction amplifications were carried out with fluorescently (6-carboxyfluorescein (FAM))–labeled reverse primers (Invitrogen). Optimal titration was defined as the point of equal signal intensity of exogenous competitor and target transcript. The resulting products were separated on a 4.5% denaturing acrylamide gel and analyzed on a semiautomated DNA Sequencer ABI 377 (Applied Biosystems, Darmstadt, Germany) using the Gene Scan Analysis Software version 3.1.

Transfection Experiments

To exogenously express *LHX9*, SF188 and KNS-42 glioma cell lines were cultured overnight on 60-mm tissue culture dishes (1×10^4) and cotransfected with a pCMV6-XL4/LHX9 plasmid containing full-length *LHX9* cDNA (2 μg) and pRS vector containing the puromycin-resistant gene (Origene, AMS Biotechnology, United Kingdom) using Lipofectamine 2000 (Invitrogen) as recommended by the protocol of the manufacturer. Cells transfected with empty plasmid vector (mock) were used as controls. After 24 hours of transfection, the cells were treated with 5 μg/ml puromycin (Sigma) for the selection of stable transfectants. After 14 days of selection, the stable cell clones (SF188-*LHX9* and KNS-42-*LHX9*) were tested for mRNA and protein expression of *LHX9* by RT-PCR and Western blot analyses and were used for further experiments. Green fluorescent protein–positive cells transfected with GFP-expressing vector were used as a control for efficiency of the transfections.

Western Blot Analysis

Nuclear extracts of puromycin-resistant SF188-*LHX9*, KNS-42-*LHX9* and mock cells (at 8.8×10^6) were prepared with a nuclear extraction kit (Active Motif SA, Rixensart, Belgium) according to the manufacturer's instructions, and protein concentration of the soluble lysates was determined using the Bradford assay. Ten micrograms of the nuclear extracts was separated by a 4% to 12% sodium dodecyl sulfate–polyacrylamide gel electrophoresis (NuPAGE; Invitrogen) under reducing conditions and were transferred to nitrocellulose membranes. The membranes were blocked with 5% bovine serum albumin in TBS–0.1% Tween 20 for 2 hours at room temperature and probed with primary antibodies at 4°C overnight. After washing, the membranes were incubated with horseradish peroxidase–conjugated secondary antibodies at room temperature for 1 hour. The primary antibodies included rabbit polyclonal antibody against Lhx9 (51 kDa; Abcam, Cambridge, United Kingdom) and anti–mouse monoclonal β-actin antibody (42 kDa; Sigma). The bound antibodies were visualized using an ECL system (Amersham Biosciences, United Kingdom).

Colony Focus Assay

A total of 1×10^4 cells were transfected three times in triplicate on 60-mm tissue culture dishes. After 24 hours of transfection, *LHX9*-transfected and mock-transfected cells were cultured in a selection medium containing 5 μg/ml puromycin for 14 days. Stable cell clones were stained with 0.1% crystal violet in 20% methanol for 10 minutes in the dark, and colonies with 50 cells or more were counted.

Cell Growth and Proliferation Assays

For the growth curve assay, a total of 1×10^4 transfected and puromycin-selected cells were plated three times in triplicate on 12-well culture plates for 24, 48, and 72 hours. Cells were harvested with 0.25% trypsin and 1 mM EDTA in medium (Invitrogen), and the number of cells was counted with a hemacytometer under microscopic observation. Results were expressed as a mean number of cells.

Glioma cell proliferation was analyzed by a 3-(4,5-dimethylthiazole-2-yl)-2,5-diphenyl tetrazolium bromide (MTT; Cell Proliferation Kit I; Roche, Mannheim, Germany) according to the manufacturer's instructions. Puromycin-resistant *LHX9*-transfected and mock-transfected cells (5×10^3) were cultured three times in triplicate on 96-well culture plates for 24, 48, and 72 hours. The cell proliferation was determined by measuring the converted formazan at 595 nm using a microplate reader (BioAnalyzer; BioTek, Bad Friedrichshall, Germany).

Transwell Cell Migration and Scratch Assays In Vitro

The migratory potential of transfected cells after puromycin selection for 14 days was estimated by a transwell migration assay as previously described [18] using transwell insert containing a 8-μm pore size polycarbonate membrane (Corning, Life Sciences, NY). Briefly, 600 μl of the medium supplemented with 10% or 20% FCS was added to the 24-well plate containing the transwell insert. For stimulation of glioma migration, the lower side of the transwell insert was precoated with 3 μg/ml of extracellular matrix (ECM) molecule vitronectin (Invitrogen) by an overnight incubation at 4°C. Cells were collected by trypsinization, resuspended in serum-free medium, plated at 1×10^4 cells/100 μl on top of the transwell membrane, and incubated at 37°C for 4 or 24 hours. Medium was then aspirated, and the cells that have migrated to the lower surface of the membrane were fixed with 4% paraformaldehyde in phosphate-buffered saline. The top of the membrane was then wiped and cleaned with a cotton swab, and the membrane was stained with hematoxylin-eosin solution. The number of migrated cells to the lower surface of the membrane was counted in four randomly selected fields of the slides under microscopic observation. Results were expressed as a percentage of migrating cells relative to the total input of cells. These experiments were performed three times in duplicate.

For the scratch assay, stable transfectants (1×10^5) were plated onto 60-mm tissue culture dishes and allowed to create a confluent monolayer. After aspirating the medium, the cell monolayer was scraped in a straight line to make a "scratch" with a 1-ml pipette tip, and cell debris were removed by washing the cells with phosphate-buffered saline. The medium supplemented with 5% FCS was added, and closure of the scratch was photographed at 0, 24, 72, and 96 hours. The number of migrating cells was determined by counting the cells that migrated into the scratch area at the indicated time points. This experiment was repeated three times in duplicate.

Matrigel Invasion Assay In Vitro

Matrigel invasion assay was performed for the evaluation of invasive capability *in vitro* by using transwell inserts containing an 8-μm pore size polycarbonate membrane (Corning, Life Sciences, NY) coated with 100 μl per well of Matrigel (Invitrogen). The puromycin-resistant transfected cells (1×10^5 cells/100 μl of serum-free medium) were plated on the top of the transwell membrane. The medium supplemented with 10% FCS was added to the 24-well plate. After 72 hours of incubation, cells that had migrated through the Matrigel and the lower surface of the membrane were fixed, stained, and counted as descried above. Results were expressed as a percentage of migrating cells relative to the total input of cells. These experiments were performed three times in duplicate.

Caspase-3 Activity

After puromycin selection for 14 days of *LHX9*-transfected and mock-transfected glioma cells, caspase-3 activity was measured using a colorimetric assay kit (CaspACE Assay System, Colorimetric; Promega) according to the manufacturer's instructions. As controls, SF188 and KNS-42 cells were treated with 0.1 to 0.5 μM staurosporine (STS) or with a combination of STS and 20 μM cell-permeable pan-caspase inhibitor Z-VAD-FMK for 24 hours. Untreated glioma cells were used as a negative control. Cell extracts were prepared by adding cell lysis buffer at a concentration of 1×10^6 cells/ml, and the protein concentration of the cell lysates was determined using Bradford assay. Twenty-five micrograms of the cell extracts and 2 μl of DEVD-pNA caspase substrate labeled with chromophore *p*-nitroaneline (pNA), which is released from the substrate upon cleavage by DEVDase, were added into 96-well plate and incubated for 4 hours at 37°C. The caspase-3 activity was determined by measuring the free pNA at 405 nm using a microplate reader (BioAnalyzer). This experiment was performed three times in duplicate.

Statistical Analysis

Data are presented as mean ± SD. Differences of the variables between groups were tested by Student's *t* test or one-way analysis of variance test, and $P \leq .05$ was considered statistically significant.

Results

Methylation Status of LHX9 *in Pediatric HGG, PA, and Glioma Cell Lines*

To investigate the role of epigenetic alterations in pediatric malignant gliomas on a genomewide scale and to identify novel genes silenced in these tumors, we performed a DMH approach that enabled us to select frequently methylated CGIs by comparing the hybridization pattern of DNA amplicons derived from tumor samples and those derived from normal tissues. We identified a novel frequently hypermethylated CGIs in about five candidate genes. Among them, a CpG-rich DNA fragment localized within the coding sequence of a *LHX9* transcript variant 2 encoding a LIM-hd transcription factor expressed in the developing brain [8,9] was found hypermethylated at the highest frequency in five of nine high-grade gliomas compared with normal brain tissue samples. Therefore, we focused on the *LHX9* gene to further verify the microarray data. First, we selected two CGI-associated regions: *LHX9* region 1 localized upstream of the transcriptional start site of *LHX9* (−1.642 to −1.303 bp) containing 22 CpG sites and *LHX9* region 2 within the coding sequence (3 intron/4 exon) of *LHX9* containing 33 CpG sites (Table 1*A* and Figure 1*A*). The 5′-*LHX9* region 1, which may possess promoter or enhancer activity, was identified by Promoter 2.0 prediction [13] and CGI searcher programs as described in the Materials and Methods section including the following criteria: CG content greater than 50, Obs CpG/Exp CpG greater than 0.60, and length of 100 bp or greater, whereas hypermethylation at *LHX9* region 2 was found by the DMH approach. We next performed bisulfite genomic sequencing to analyze the methylation levels of the 22 CpG positions within *LHX9* region 1 in a subset of nine pediatric high-grade astrocytic tumors analyzed by DMH. Nontumorous pediatric brain samples were used as controls. Analysis of bisulfite-modified DNA by BiQ Analyzer Software [14] showed that the 339-bp upstream fragment 1 of *LHX9* was unmethylated (≤2%) in normal pediatric brain tissues, whereas extensive methylation of all CpG sites was observed in one glioblastoma sample (Figure 1*B*) and a partial methylation of all CpG sites was found in two tumor samples whereas one astrocytic tumor showed evidence of methylation of a limited number of CpG sites (5%). The remaining five glioma samples were unmethylated at all CpG sites assessed. These findings demonstrated that four of the five HGGs exhibiting hypermethylation at region 2 within *LHX9* also showed *de novo* methylation at region 1 by bisulfite sequencing.

Using a COBRA approach [19], we also wanted to quantitatively estimate the aberrant DNA methylation status of the two selected CpG-rich regions of *LHX9* gene in a larger set of 25 pediatric HGGs and 3 normal brain control samples, including those samples that have been analyzed by DMH, and 4 pediatric glioma cell lines (CHLA-200, SF188, KNS-42, and KG-1-C). *De novo* DNA methylation at the two *Bst*UI restriction sites of *LHX9* region 1 was detected in 28% (7/25 cases; Figure 1*B*) of the pediatric HGG samples and quantified to an average of 20% methylated alleles compared with the three nonpathological brain tissue samples that were unmethylated. Glioma cell lines SF188 and KNS-42 were completely methylated exhibiting an average of 98.5% methylated alleles, whereas CHLA-200 and KG-1-C cell lines were unmethylated at the *Bst*UI restriction sites of *LHX9* fragment 1 (Figure 1*B*). To analyze the methylation status of the second *LHX9* region, we used a nested PCR and a combination of two restriction endonucleases, *Bst*UI and *Taq*$^{\alpha}$I, and could therefore assess DNA methylation at 6 of 33 CpG sites. The COBRA approach of the two overlapping PCR products of *LHX9* region 2 revealed *de novo* methylation at all restriction sites in 88% (22/25 tumor samples) of pediatric HGGs and in the four glioma cell lines and assessed to an average of 51% methylated alleles and an average of 87% methylated alleles, respectively, in comparison to the unmethylated normal brain tissue samples (Figure 1*C*). These results demonstrated a frequent hypermethylation of the second CGI-associated region compared with the first upstream putative promoter region of the *LHX9* gene and with the normal brain tissue samples that were unmethylated. Taken together, our data showed that the second *LHX9* fragment seems to be a critical target for DNA methylation in pediatric HGGs.

To examine whether *LHX9* gene is also hypermethylated in pediatric low-grade gliomas, we analyzed the methylation profile of *LHX9* in 14 pediatric PAs (WHO grade 1). The DNA methylation status of the second CpG-rich *LHX9* region, as it was more frequently methylated in pediatric HGGs, was estimated by COBRA approach. *De novo* methylation of a limited number of CpG positions at the *LHX9* region 2 was detected in 29% (4/14 cases; Figure 1*C*) of tumor samples and quantified to an average of 10% methylated alleles, indicating a much lower level of methylation of *LHX9* in pediatric PAs compared with that of HGGs.

Expression Analysis of LHX9 *Gene in HGG, PA, and Glioma Cell Lines*

To determine the transcriptional expression levels of *LHX9* in 11 pediatric HGGs and 1 nontumorous pediatric brain sample for which total RNA was available, we carried out cRT-PCR using specific RNA competitor molecules for *LHX9* and the housekeeping gene *β-actin*. cDNA samples derived from normal testis were used as a positive control [20] for *LHX9* gene expression (data not shown). The four glioma cell lines were also analyzed. *LHX9* expression was determined by a titration of the constant amount of total RNA against serial dilutions of exogenous competitor RNA and normalized to the transcript levels of constitutively expressed *β-actin*. The cRT-PCR analysis showed that the relative *LHX9* mRNA levels were markedly reduced in 8 (73%) of 11 tumor samples (an average of 15-fold reduction) and in all glioma cell lines (an average of 40-fold reduction) compared with the *LHX9* mRNA level in normal brain tissue sample (Figure 2*A*). Three gliomas displayed high *LHX9* expression but lower than that of the normal brain. To examine whether the CGI hypermethylation affects the expression of *LHX9*, we next correlated methylation status with transcript levels of *LHX9*. From the 11 HGGs analyzed, 8 tumor samples with extensive methylation at *LHX9* region 1 or region 2 showed low *LHX9* mRNA expression, whereas 1 tumor sample with limited methylation and 2 cases without methylation at *LHX9* displayed high expression levels. All four glioma cell lines with hypermethylated *LHX9* pattern showed reduced *LHX9* mRNA levels. These data indicated a significant correlation ($P < .0001$) between hypermethylation and decreased or weak expression of *LHX9* in HGGs and cell lines (Figure 2*A*, *scatter plot*).

Analysis of the relative *LHX9* mRNA levels in the four only partially methylated PAs revealed a four-fold lower *LHX9* expression compared with normal brain but approximately a four-fold higher transcriptional level compared with that in extensively methylated HGGs (Figure 2*A*). Together, these results demonstrated that the *LHX9* gene was less DNA-methylated in pediatric noninvasive pilocytic astrocytomas compared with HGGs, indicating an inverse correlation between degree of methylation and mRNA expression in gliomas.

Effect of Treatment of Glioma Cell Lines with a Demethylating Agent

To estimate if the observed reduction of expression in HGGs is associated with CGI hypermethylation of the *LHX9* gene, the transcript levels and DNA methylation status of *LHX9* were analyzed in

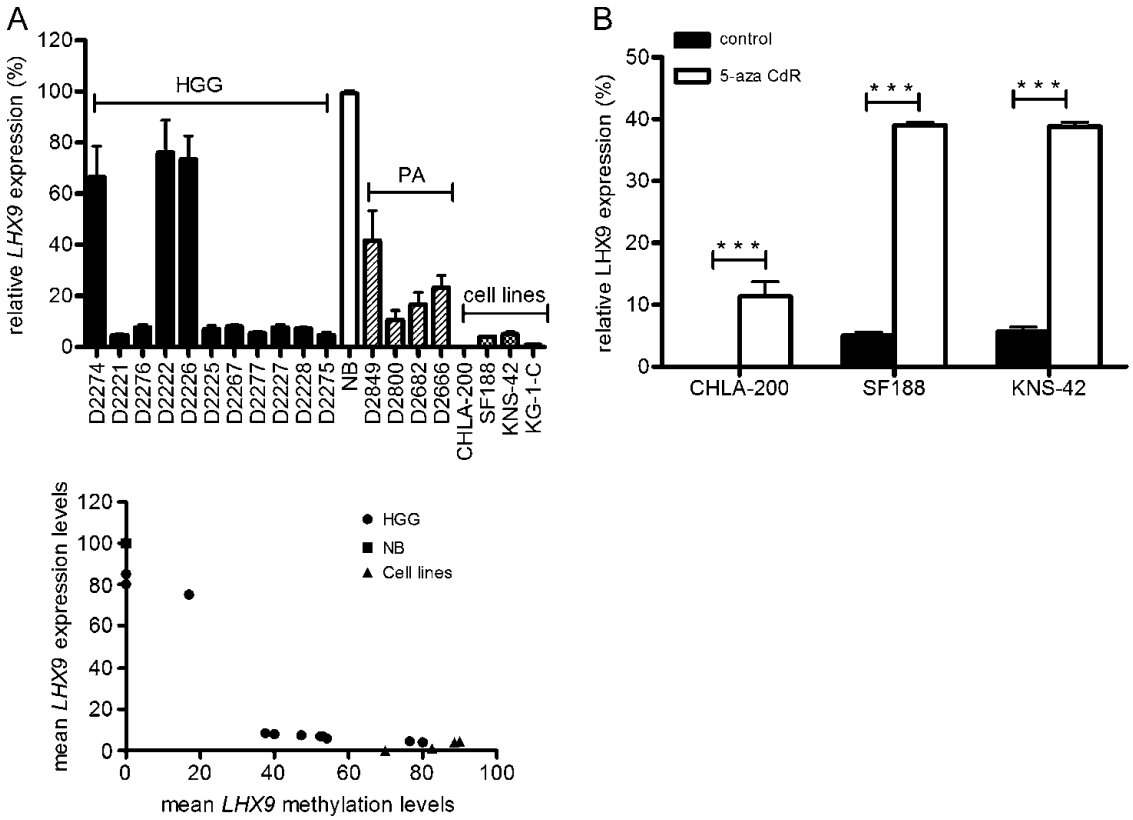

Figure 2. *LHX9* mRNA expression in pediatric HGG, PA, and glioma cell lines. *LHX9* expression levels were estimated by cRT-PCR in (A) tumor samples and cell lines and (B) glioma cell lines before and after treatment with the demethylating agent 5-aza CdR. *LHX9*- specific mRNA levels were quantified by titrating 250 ng of target RNA against serial dilutions of exogenous competitor RNA ranging from 0.8 to 150 pg and normalized to the transcript levels of constitutively expressed *β-actin*. (A) The cRT-PCR analysis showed that the relative *LHX9* mRNA levels in HGG were markedly reduced in 8 (73%) of 11 tumor samples and in all 4 glioma cell lines compared with the *LHX9* mRNA level in normal brain control sample (NB). *LHX9* expression in PA was lower than in NB but not silenced as it is shown for the 8 of 11 HGGs and the glioma cell lines. Scatter plot represents a significant correlation ($P < .0001$) between hypermethylation and decreased expression of *LHX9* in HGG and glioma cell lines. (B) Comparison of the expression pattern of *LHX9* treated with 5-aza CdR and untreated glioma cell lines demonstrated that the transcription level in treated cells was significantly increased: $^{***}P < .0001$. Data represent the means ± SD of three independent experiments.

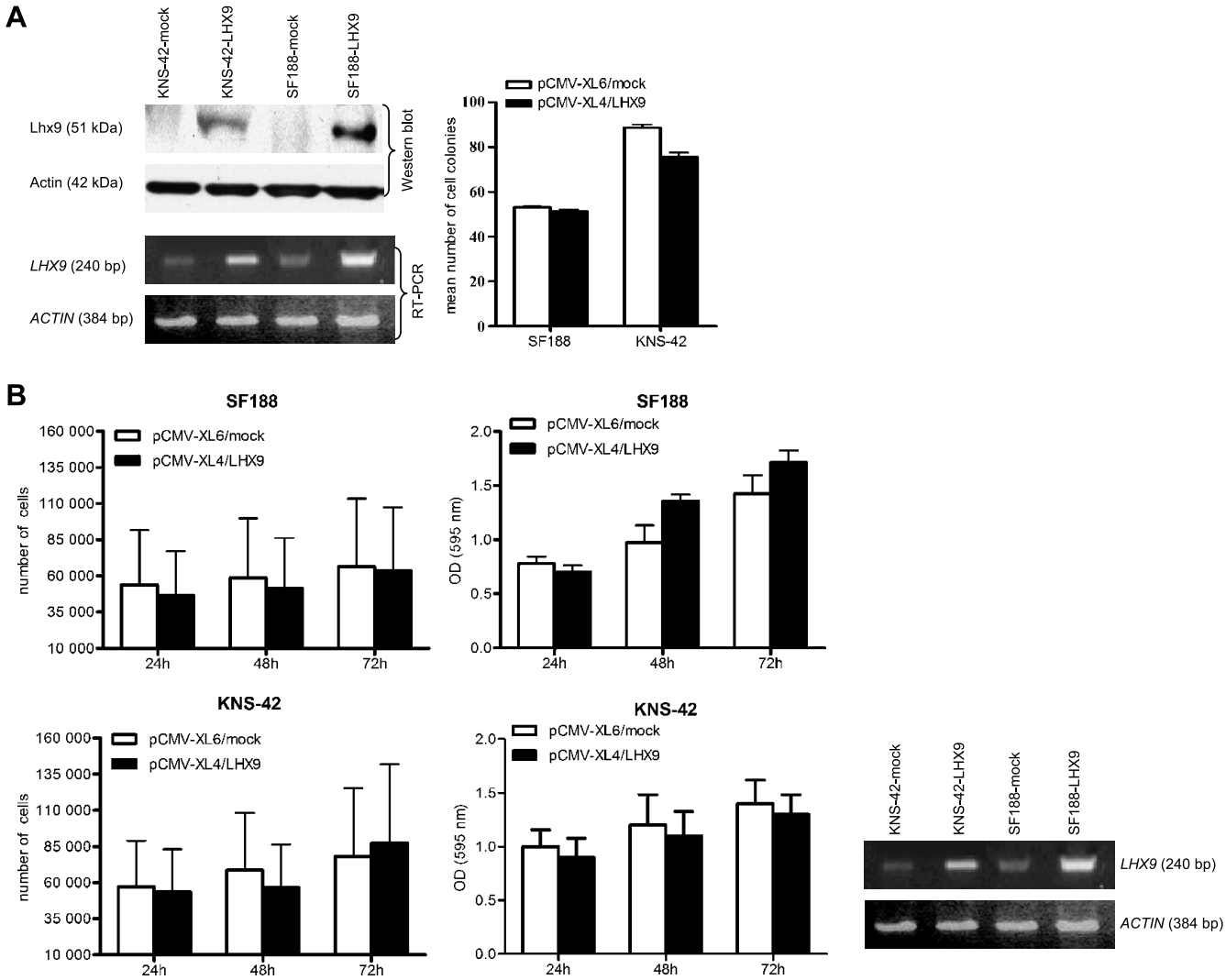

Figure 3. Reexpression of *LHX9* does not affect glioma cell growth. (A) Colony formation and (B) cell growth and proliferation assays were performed after transfection with pCMV-XL4/LHX9 or empty vector (pCMV-XL6/mock) and puromycin selection for 14 days. (A) Protein and mRNA overexpression of *LHX9* in two pediatric glioma cell lines (SF188 and KNS-42) after transfection, and puromycin selection was tested by Western blot analysis and RT-PCR. Western blot represents nuclear extracts of the stable transfectants probed with antibody against Lhx9. *LHX9* mRNA levels of puromycin-resistant transfected cells were assessed by RT-PCR. Equal loading was confirmed by β-actin. Subsequently, stable transfectants were stained with 0.1% crystal violet in 20% methanol for colony formation assay, and colonies with 50 cells or more were counted. (B) Growth of the puromycin-resistant *LHX9*-transfected or mock-transfected glioma cells was assessed by counting the cells after 24, 48, and 72 hours of incubation at 37°C. Results were expressed as a mean number of cells. Proliferation activity of the stable cell clones was also characterized by the MTT assay. The cell proliferation was determined after 24, 48, and 72 hours of incubation at 37°C by measuring the converted formazan at 595 nm using a microplate reader. *LHX9* overexpression in stable transfectants was tested by RT-PCR analysis for each of the experiments performed. Data represent the means ± SD of at least three independent experiments done in triplicate.

three glioma cell lines (CHLA-200, SF188, and KNS-42) before and after treatment with the DNA methyltransferase inhibitor 5-aza CdR (5 μM) for 4 days. The mRNA levels of *LHX9* were assessed by cRT-PCR (Figure 2*B*). The DNA methylation status of CpG-rich *LHX9* region 2 in the cells before and after treatment with demethylating agent was analyzed by COBRA (Figure 1*C*). To verify the effect of 5-aza CdR treatment in our experiment, we examined the expression level of a *PCDH-γ-A11* gene, which is known to be silenced by methylation in glioma cells [16]. The RT-PCR analysis showed that exposure of glioma cells to 5 μM 5-aza CdR induced reexpression of *PCDH-γ-A11*, confirming that demethylation using 5-aza CdR was able to restore the expression from a promoter known to be silenced by aberrant methylation in these cells (data not shown). Comparison of the expression pattern of *LHX9* in glioma cells incubated with or without 5 μM 5-aza CdR demonstrated that the *LHX9* transcription level in treated cells was increased to 12.5-fold (Figure 2*B*). In contrast, the relative mRNA level of *LHX9* in treated glioma cells was still lower than that in the normal brain tissue sample and assessed to an average of 30% expression. The COBRA assay showed that the methylation of the *Bst*UI restriction site at the CGI-associated region 2 of *LHX9* was reduced in cells after 5-aza CdR treatment in comparison to untreated cells, indicating that the examined hypermethylation of the *LHX9* fragment 2 was reversible and may have contributed to reduced expression of *LHX9*.

Reexpression of LHX9 *Does Not Affect Glioma Cell Growth*

To assess the functional role of *LHX9* in pediatric HGGs, we overexpressed *LHX9* in two pediatric glioma cell lines (SF188 and KNS-42). After puromycin selection for 14 days, mRNA and protein overexpression of *LHX9* was confirmed by RT-PCR and Western blot analyses (Figure 3*A*), and stable clones were used for further experiments. Glioma growth activity in puromycin-resistant transfectants was determined by colony focus and proliferation assays. Colony focus assay revealed similar numbers of colonies in both *LHX9*-transfected (SF188-*LHX9* and KNS-42-*LHX9*) and mock-transfected cells (Figure 3*A*). Comparison of the proliferation activity of *LHX9*-transfected and mock glioma cells using cell growth and MTT assays revealed no significant differences at the three time points analyzed ($P \geq .05$; Figure 3*B*). These results demonstrated that the overexpression of *LHX9* did not suppress glioma cell growth suggesting that epigenetic modification of *LHX9* expression does not affect glioma cell proliferation.

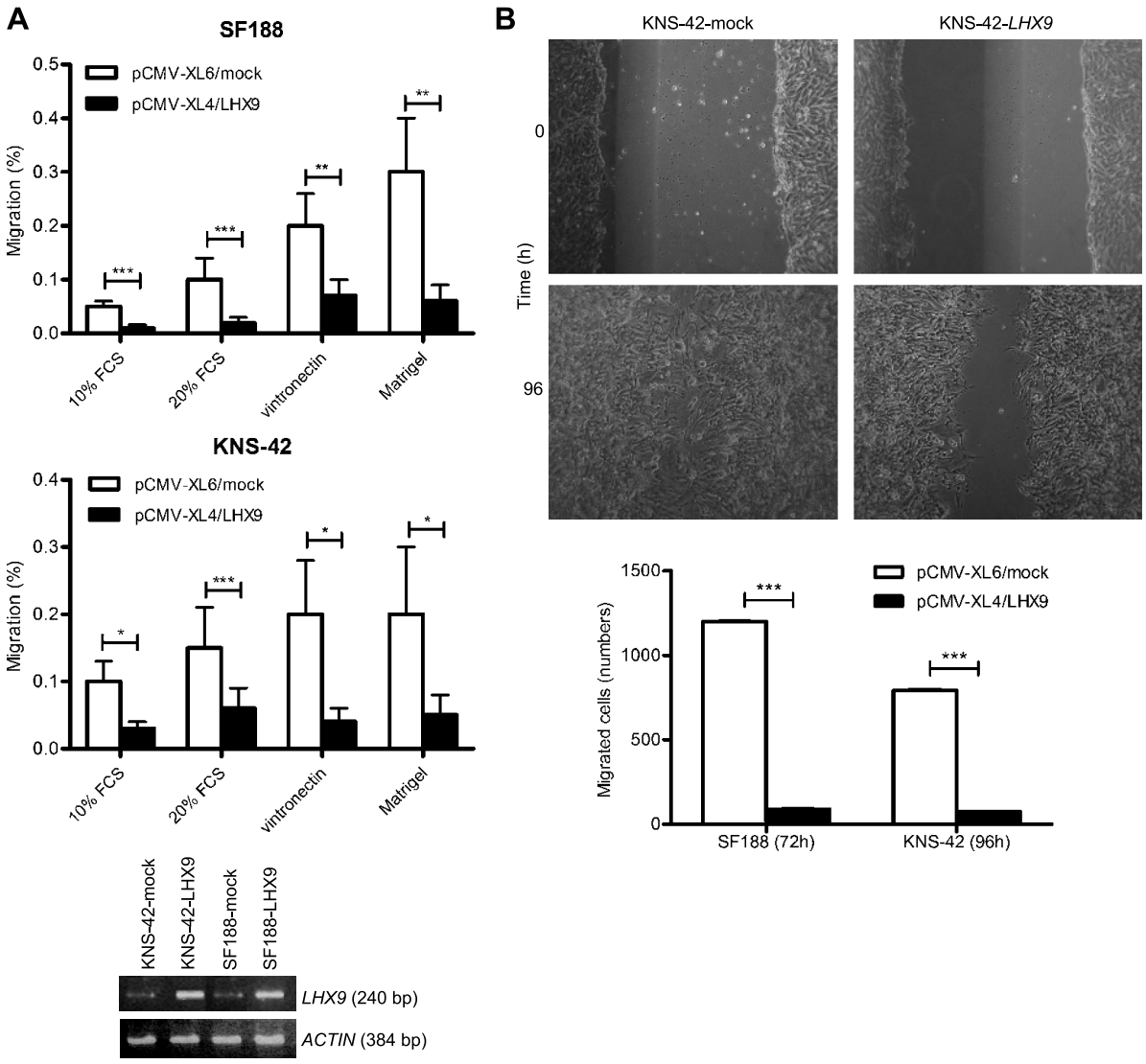

Figure 4. Reexpression of *LHX9* inhibits glioma cell migration and invasion *in vitro*. Transwell migration, invasion (A), and scratch (B) assays of the puromycin-resistant *LHX9*-transfected and mock-transfected glioma cell lines SF188 and KNS-42. (A) Transwell migration and invasion of *LHX9*-transfected glioma cells was significantly inhibited compared to mock-transfected cells both, in the presence of 10% (***P = .0006 for SF188, *P = .01 for KNS-42) or 20% FCS (***P = .0008 for SF188, ***P = .0003 for KNS-42) in the medium after 24 hours of incubation. Coating the lower side of the transwell insert with ECM molecule vitronectin (**P = .005 for SF188, *P = .01 for KNS-42) or with Matrigel (**P = 0084 for SF188, *P = .01 for KNS-42) significantly stimulated the migration or invasion of mock-transfected cells after 72 hours of incubation compared with *LHX9*-transfected cells. *LHX9* overexpression in stable transfectants was confirmed by RT-PCR analysis for each of the experiments performed. (B) Confluent monolayers of KNS-42-*LHX9*–transfected and KNS-42 mock-transfected glioma cells were scratched, and the complete closure of the scratch was achieved after 96 hours and photographed. Note that the mock-transfected glioma cells migrated and covered the scratch, whereas a significant area of the scratch remains uncovered in *LHX9*-transfected cells. Similar results were observed for the SF188-transfected cell clones (see the graph). The number of migrating cells was determined by counting the cells that migrated into the scratch area at the indicated time points (***$P < .0001$). Data represent the means ± SD of three independent experiments done in duplicates.

LHX9 *Overexpression Inhibits Glioma Cell Migration and Invasion But Does Not Induce Apoptosis*

To investigate whether *LHX9* expression is involved in glioma cell migration, we performed transwell migration and scratch assays *in vitro*. Transwell migration assay represented an *in vitro* model for invasive migration. As shown in Figure 4*A*, reexpression of *LHX9* significantly decreased the migratory potential of the stable *LHX9*-transfected cell clones through the transwell membrane compared with the mock-transfected cells. Coating the lower side of the transwell insert with the ECM molecule vitronectin significantly stimulated the migration of glioma cells. However, the mock-transfected cells again showed a higher migratory activity compared with the *LHX9*-transfected cells (Figure 4*A*). A similar result was observed during evaluation of the migratory ability of the glioma cells using a scratch assay *in vitro*. As shown in Figure 4*B*, KNS-42-mock and SF188-mock cells migrated and completely closed the scratch after 96 and 72 hours, respectively, whereas the significant area of the scratch remained uncovered in KNS-42-*LHX9* and SF188-*LHX9* cells. Together, these findings showed that *LHX9* expression may impact the migration of pediatric glioma cells.

To further support the role of *LHX9* in the invasive behavior of glioma cells, we performed an invasion assay using Matrigel, a basement membrane matrix containing laminin, collagen IV, entactin, and heparin sulfate proteoglycan. Again, an exogenous expression of *LHX9* in the stable transfectants resulted in a significant reduction of invasion through Matrigel compared with the mock-transfected cells (Figure 4*A*) indicating that *LHX9* plays a specific role in pediatric glioma cell invasion.

On the basis of the previous data showing a direct correlation between invasion and apoptosis resistance in malignant gliomas [21], we measured caspase-3 activity of puromycin-resistant *LHX9*-transfected and mock cells to determine whether the exogenous *LHX9* expression in these cells may directly induce apoptosis. We were not able to detect a significant number of cells that were undergoing apoptosis (Figure 5) indicating that *LHX9* expression is not directly involved in the induction of apoptosis in pediatric glioma cells.

Discussion

In the current study, we provide evidence that *LHX9* (human LIM-hd 9 transcription factor) is not only frequently hypermethylated in pediatric malignant astrocytomas but that this epigenetic alteration of the *LHX9* gene is associated with reduced mRNA expression and is involved in the migratory and invasive phenotype of glioma cells in a tumor-specific manner.

LHX9 belongs to a family of LIM-hd transcription factors containing a DNA-binding domain and two highly conserved cystein-rich zinc-binding domains involved in protein-protein interactions [22,23]. The roles of the LIM-hd–encoding genes have been mostly defined in the context of nervous system development where they are critically involved in cell determination [24]. Although it is known that *LHX9* is strongly expressed in embryonic mouse brain, its expression in brain tumors has not yet been a matter of investigation. Using DMH, bisulfite sequencing, and COBRA assays, we examined for the first time the DNA methylation status and the expression profile of *LHX9* in pediatric astrocytic tumors. Other LIM-hd factors have been shown to exhibit an epigenetic transcriptional regulation and have been implicated in tumorigenesis. For instance, the *LHX6* gene has been found to be a sensitive DNA methylation biomarker in head and neck carcinomas [25]. Recent data using gene expression profiling have identified an increased expression of *LHX2* in PAs and ependymomas as well as in normal murine astrocytes and neural stem cells [26]. As far as we are aware, *LHX9* hypermethylation and expression have not been previously investigated in astrocytomas or other tumor types.

Because down-regulation of gene expression through promoter hypermethylation has been reported to be an important mechanism of transcriptional silencing in many tumors [27], we focused to examine 1) the DNA methylation status of two *LHX9* CpG-rich regions and 2) the possible functional implication of methylation on *LHX9* expression in pediatric high-grade astrocytomas. We established a COBRA assay using the restriction endonuclease *Bst*UI or a combination of the two restriction endonucleases *Bst*UI and *Taq*$^{\alpha}$I to analyze the methylation status of the two CGI-associated *LHX9* regions in 39 pediatric tumor

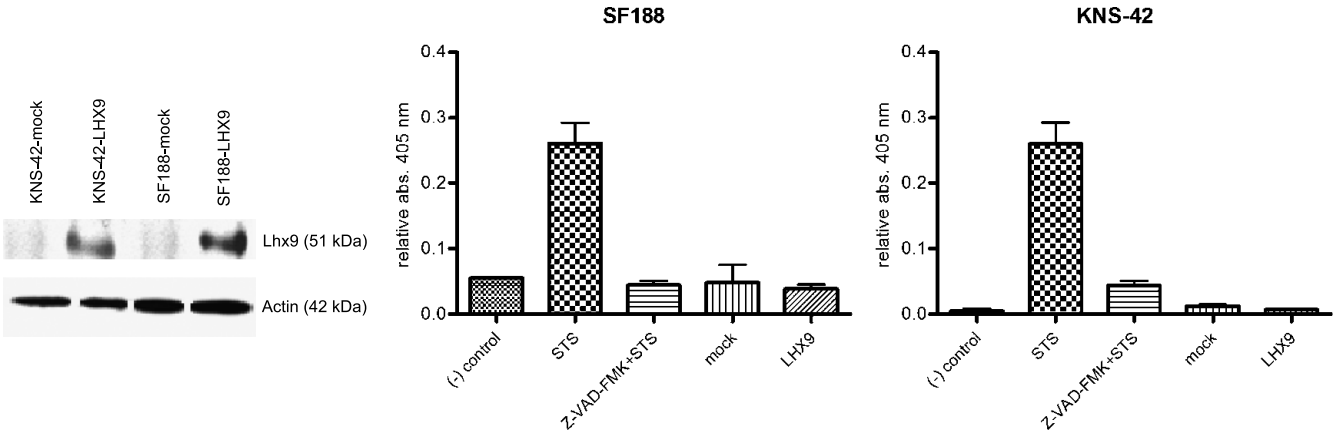

Figure 5. Reexpression of *LHX9* does not induce apoptosis. Apoptosis in *LHX9*-transfected and mock-transfected glioma cells was assessed by measuring the caspase-3 activity after 14 days of selection with puromycin. *LHX9* overexpression was confirmed by Western blot analysis. Cells lysates treated with STS were used as a positively induced apoptosis control, whereas cells lysates treated with a combination of STS and cell-permeable pan-caspase inhibitor Z-VAD-FMK (Z-VAD-FMK + STS) were set up as an inhibited apoptosis control. Untreated glioma cells were used as a negative control ((−) control). The caspase-3 activity was determined by measuring the free pNA at 405 nm using a microplate reader (see Materials and Methods). Both the *LHX9*-transfected (SF188-LHX9 and KNS-42-LHX9) and the mock-transfected (SF188-mock and KNS-42-mock) cells did not induce apoptosis. Data represent the means ± SD of three independent experiments done in duplicate.

cases, 3 normal brain control samples, and 4 pediatric glioma cell lines. Our results demonstrated that the second CGI-associated region within *LHX9* seems to be a critical target for DNA methylation because it was more frequently hypermethylated in most of the HGGs and glioma cell lines. Moreover, our data suggest a potential association between hypermethylation at CpG-rich region 2 and reduced mRNA expression of the *LHX9* transcript variant 2 in pediatric malignant astrocytic tumors and glioma cell lines as we found that glioma samples exhibiting hypermethylation at this *LHX9* fragment expressed decreased transcript levels relative to unmethylated normal brain tissue and that treatment of glioma cells with the demethylating reagent (5-aza CdR) restored *LHX9* mRNA expression. The undigested *LHX9* band observed in some of the samples treated with the restriction endonucleases may represent unmethylated alleles in the tumors and thus may reflect a cellular heterogeneity of high-grade astrocytomas. Because PAs are low-grade nondiffuse gliomas that lack the typical molecular alterations associated with diffuse high-grade astrocytomas [28,29] and expressed a large number of genes involved in brain development [30,31], we also analyzed the methylation profile of *LHX9* in these tumors and found that the CpG-rich fragment within the coding sequence of *LHX9* gene was methylated to a limited extend. These results clearly demonstrated that hypermethylation of *LHX9* represents a frequent and tumor-specific event in pediatric malignant astrocytomas and may contribute to their tumor biology. Furthermore, hypermethylation of the CpG-rich *LHX9* regions was not a feature of normal pediatric brain tissues as we showed by bisulfite sequencing and COBRA, and it likely represents a tumor-associated event that occurs *de novo* in the development of pediatric astrocytic tumors.

Exogenous expression of *LHX9* in pediatric glioma cell lines exhibiting extensive methylation of the CGI-associated *LHX9* regions did not affect glioma cell growth and apoptosis but significantly decreased cell motility and invasive behavior *in vitro* indicating that this gene is specifically involved in glioma cell migration and invasion. A number of genes known to be involved in cell motility and adhesion are deregulated in invasive and metastatic cancer cells, and alteration of the expression patters of these genes can promote or suppress cancer cell invasiveness and metastasis [32]. As invasive behavior is a hallmark of HGGs, our results suggest that the epigenetic modification of *LHX9* expression promotes glioma cell motility, whereas reexpression of this gene in extensively methylated cells suppressed cell migration and invasion indicating that *LHX9* silencing may contribute to the migratory and invasive phenotype of glioma cells.

On the basis of the previous data that showed high degree of homology between the LIM domains of Lhx9 and those of Lhx2 and coexpression of these two genes in numerous regions of the developing brain [8] and that increased expression of *LHX2* was detected in PAs [26], we suggested that *LHX9* may also be expressed by these benign, nondiffuse gliomas. Our results showed a lack of silencing by DNA methylation of the *LHX9* gene in PAs. This may be directly related to the noninvasive behavior of these tumors. Further work such as identification of transcriptional targets of *LHX9* has to elucidate the specific role of *LHX9* in pediatric tumor progression and brain invasion.

In summary, we have identified frequent hypermethylation of a CGI-associated region of the *LHX9* gene in pediatric malignant astrocytomas associated with reduced *LHX9* gene expression. Reexpression of *LHX9* suppressed glioma migration and invasion without directly affecting proliferation or apoptosis, suggesting that the frequent epigenetic silencing of the *LHX9* gene is implicated in the invasive behavior of pediatric HGGs. Further studies of the mechanism(s) by which *LHX9* mediates glioma cell migration and invasiveness will contribute to a better understanding of its role in glioma biology.

References

[1] Rickert CH, Strater R, Kaatsch P, Wassmann H, Jurgens H, Dockhorn-Dworniczak B, and Paulus W (2001). Pediatric high-grade astrocytomas show chromosomal imbalances distinct from adult cases. *Am J Pathol* **158**, 1525–1532.

[2] Belinsky SA (2004). Gene-promoter hypermethylation as a biomarker in lung cancer. *Nat Rev Cancer* **4**, 707–717.

[3] Stone AR, Bobo W, Brat DJ, Devi NS, Van Meir EG, and Vertino PM (2004). Aberrant methylation and down-regulation of TMS1/ASC in human glioblastoma. *Am J Pathol* **165**, 1151–1161.

[4] Costello JF, Plass C, and Cavenee WK (2000). Aberrant methylation of genes in low-grade astrocytomas. *Brain Tumor Pathol* **17**, 49–56.

[5] Kim TY, Zhong S, Fields CR, Kim JH, and Robertson KD (2006). Epigenomic profiling reveals novel and frequent targets of aberrant DNA methylation–mediated silencing in malignant glioma. *Cancer Res* **66**, 7490–7501.

[6] Costello JF (2003). DNA methylation in brain development and gliomagenesis. *Front Biosci* **8**, s175–s184.

[7] Yan PS, Chen CM, Shi H, Rahmatpanah F, Wei SH, Caldwell CW, and Huang TH (2001). Dissecting complex epigenetic alterations in breast cancer using CpG island microarrays. *Cancer Res* **61**, 8375–8380.

[8] Retaux S, Rogard M, Bach I, Failli V, and Besson MJ (1999). *Lhx9*: a novel LIM-homeodomain gene expressed in the developing forebrain. *J Neurosci* **19**, 783–793.

[9] Failli V, Rogard M, Mattei MG, Vernier P, and Retaux S (2000). Lhx9 and Lhx9alpha LIM-homeodomain factors: genomic structure, expression patterns, chromosomal localization, and phylogenetic analysis. *Genomics* **64**, 307–317.

[10] Louis DN, Ohgaki H, Wiestler OD, Cavenee WK, Burger PC, Jouvet A, Scheithauer BW, and Kleihues P (Eds.) (2007). WHO Classification of tumors of the central nervous system. IARC, Lyon, France.

[11] Wolff JE, Wagner S, Reinert C, Gnekow A, Kortmann RD, Kuhl J, and Van Gool SW (2006). Maintenance treatment with interferon-gamma and low-dose cyclophosphamide for pediatric high-grade glioma. *J Neurooncol* **79**, 315–321.

[12] Huang TH, Perry MR, and Laux DE (1999). Methylation profiling of CpG islands in human breast cancer cells. *Hum Mol Genet* **8**, 459–470.

[13] Knudsen S (1999). Promoter2.0: for the recognition of PolII promoter sequences. *Bioinformatics* **15**, 356–361.

[14] Bock C, Reither S, Mikeska T, Paulsen M, Walter J, and Lengauer T (2005). BiQ Analyzer: visualization and quality control for DNA methylation data from bisulfite sequencing. *Bioinformatics* **21**, 4067–4068.

[15] Mikeska T, Bock C, El-Maarri O, Hubner A, Ehrentraut D, Schramm J, Felsberg J, Kahl P, Buttner R, Pietsch T, et al. (2007). Optimization of quantitative MGMT promoter methylation analysis using pyrosequencing and combined bisulfite restriction analysis. *J Mol Diagn* **9**, 368–381.

[16] Waha A, Guntner S, Huang TH, Yan PS, Arslan B, Pietsch T, and Wiestler OD (2005). Epigenetic silencing of the protocadherin family member PCDH-gamma-A11 in astrocytomas. *Neoplasia* **7**, 193–199.

[17] Waha A, Watzka M, Koch A, Pietsch T, Przkora R, Peters N, Wiestler OD, and von Deimling A (1998). A rapid and sensitive protocol for competitive reverse transcriptase (cRT) PCR analysis of cellular genes. *Brain Pathol* **8**, 13–18.

[18] Scheef EA, Huang Q, Wang S, Sorenson CM, and Sheibani N (2007). Isolation and characterization of corneal endothelial cells from wild type and thrombospondin-1 deficient mice. *Mol Vis* **13**, 1483–1495.

[19] Xiong Z and Laird PW (1997). COBRA: a sensitive and quantitative DNA methylation assay. *Nucleic Acids Res* **25**, 2532–2534.

[20] Mazaud S, Oreal E, Guigon CJ, Carre-Eusebe D, and Magre S (2002). Lhx9 expression during gonadal morphogenesis as related to the state of cell differentiation. *Gene Expr Patterns* **2**, 373–377.

[21] Hoelzinger DB, Mariani L, Weis J, Woyke T, Berens TJ, McDonough WS, Sloan A, Coons SW, and Berens ME (2005). Gene expression profile of glioblastoma multiforme invasive phenotype points to new therapeutic targets. *Neoplasia* **7**, 7–16.

[22] Sanchez-Garcia I and Rabbitts TH (1994). The LIM domain: a new structural motif found in zinc-finger–like proteins. *Trends Genet* **10**, 315–320.

[23] Dawid IB, Toyama R, and Taira M (1995). LIM domain proteins. *C R Acad Sci III* **318**, 295–306.

[24] Curtiss J and Heilig JS (1998). DeLIMiting development. *Bioessays* **20**, 58–69.

[25] Estecio MR, Youssef EM, Rahal P, Fukuyama EE, Gois-Filho JF, Maniglia JV, Goloni-Bertollo EM, Issa JP, and Tajara EH (2006). LHX6 is a sensitive methylation marker in head and neck carcinomas. *Oncogene* **25**, 5018–5026.

[26] Sharma MK, Mansur DB, Reifenberger G, Perry A, Leonard JR, Aldape KD, Albin MG, Emnett RJ, Loeser S, Watson MA, et al. (2007). Distinct genetic signatures among pilocytic astrocytomas relate to their brain region origin. *Cancer Res* **67**, 890–900.

[27] Karpf AR and Jones DA (2002). Reactivating the expression of methylation silenced genes in human cancer. *Oncogene* **21**, 5496–5503.

[28] Hunter S, Young A, Olson J, Brat DJ, Bowers G, Wilcox JN, Jaye D, Mendrinos S, and Neish A (2002). Differential expression between pilocytic and anaplastic astrocytomas: identification of apolipoprotein D as a marker for low-grade, non-infiltrating primary CNS neoplasms. *J Neuropathol Exp Neurol* **61**, 275–281.

[29] Rickman DS, Bobek MP, Misek DE, Kuick R, Blaivas M, Kurnit DM, Taylor J, and Hanash SM (2001). Distinctive molecular profiles of high-grade and low-grade gliomas based on oligonucleotide microarray analysis. *Cancer Res* **61**, 6885–6891.

[30] Gutmann DH, Hedrick NM, Li J, Nagarajan R, Perry A, and Watson MA (2002). Comparative gene expression profile analysis of neurofibromatosis 1–associated and sporadic pilocytic astrocytomas. *Cancer Res* **62**, 2085–2091.

[31] Wong KK, Chang YM, Tsang YT, Perlaky L, Su J, Adesina A, Armstrong DL, Bhattacharjee M, Dauser R, Blaney SM, et al. (2005). Expression analysis of juvenile pilocytic astrocytomas by oligonucleotide microarray reveals two potential subgroups. *Cancer Res* **65**, 76–84.

[32] Sahai E (2005). Mechanisms of cancer cell invasion. *Curr Opin Genet Dev* **15**, 87–96.